

The SwaNNFlight System: On-the-Fly Sim-to-Real Adaptation via Anchored Learning

Bassel El Mabsout^{*1}, Shahin Roozkhosh^{*1}, Siddharth Mysore¹, Kate Saenko^{1,2} and Renato Mancuso¹

Abstract—Reinforcement Learning (RL) agents trained in simulated environments and then deployed in the real world are often sensitive to the differences in dynamics presented, commonly termed the sim-to-real gap. With the goal of minimizing this gap on resource-constrained embedded systems, we train and live-adapt agents on quadrotors built from off-the-shelf hardware. In achieving this we developed three novel contributions. (i) SwaNNFlight, an open-source firmware enabling wireless data capture and transfer of agents’ observations. Fine-tuning agents with new data, and receiving and swapping onboard NN controllers – all while in flight. We also design SwaNNFlight System (SwaNNFS) allowing new research in training and live-adapting learning agents on similar systems. (ii) Multiplicative value composition, a technique for preserving the importance of each policy optimization criterion, improving training performance and variability in learnt behavior. And (iii) anchor critics to help stabilize the fine-tuning of agents during sim-to-real transfer, online learning from real data while retaining behavior optimized in simulation. We train consistently flight-worthy control policies in simulation and deploy them on real quadrotors. We then achieve ‘live’ controller adaptation via over-the-air updates of the onboard control policy from a ground station. Our results indicate that live adaptation unlocks a near-50% reduction in power consumption, attributed to the sim-to-real gap. Finally, we tackle the issues of catastrophic forgetting and controller instability, showing the effectiveness of our novel methods. Project Website: <https://github.com/BU-Cyber-Physical-Systems-Lab/SwaNNFS>

I. INTRODUCTION

Reinforcement Learning (RL) enables training policies to solve complex control problems for which traditional techniques may be ill-equipped. RL agents are often trained and evaluated in simulated environments. However, recent work has shown that these controllers applied to real systems can exhibit undesirable properties ranging from minor jerkiness, to over-heating due to the high power consumption of inefficient control policies, and even to hardware failures [1]–[5]. These problems can be attributed to a failure of control policies to cross the domain gap between simulated training environments and the real world, i.e. the *reality gap*. Despite this, simulated training remains attractive because direct on-robot training raises important safety and scalability concerns. Mobile robots often need to minimize size, weight, and power consumption (SWaP) and the resource-intensity of iteratively training controllers to adapt to the real-world may be untenable on embedded micro-controllers. SWaP considerations may preclude on-device training of controllers but relying on a more powerful ground station for training and

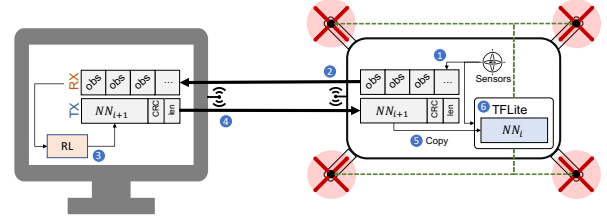


Fig. 1: SwaNNFS System overview for live adaptation. 1) Observations received as a result of policy invocation are packaged and 2) sent to the ground-station where they are unpacked and fed into an RL algorithm. 3) The updated policy is packaged with integrity check markers and 4) transmitted to the drone. 5) Upon verification of the received policy graph, the new graph is copied to system memory and 6) interpreted by TFLite for invocation.

inference of the control logic limits the robots’ practicality and makes them unusable upon communication failure.

Contribution: (i) First, we introduce an updated open-source flight control firmware, Swappable Neural Network Flight control (SwaNNFlight), and a corresponding framework SwaNNFS. We build upon prior work on Neuroflight developed by Koch et al. [6], [7], which provides a system for training and deploying neural-networks (NN) for drone control. Unfortunately, their method of including NN controllers into the firmware using TensorFlow-v1 (TF1) tools prevents swapping NN models during live operation. SwaNNFlight is rebuilt to support TensorFlow-v2 (TF2) and provide primitives for the transmission and receipt of observation data and full neural networks during flight. SwaNNFS enables training updated NN controllers with data acquired during flight and controller hot-swapping to seamlessly update NN controllers mid-flight. However, when attempting to train agents and live-adapting them with traditional RL methods, we observed problems such as low performance, catastrophic forgetting, and complete loss of control. We attribute these to the high variance in the quality of policies learned in simulation, and the biased distribution of data captured in real flight, which motivated our next two contributions. (ii) We combat training variance by multiplicatively composing policy optimization criteria, instead of linearly, thus substantially improving learning performance. (iii) To tackle the data diversity problem, we introduce *anchor critics* for live adaptation, where the value function learned in simulation is preserved and used in tandem with a value function learned on data gathered on-robot. This demonstrably improves behavior retention while still allowing policies to adapt to new data, resulting in improved control with 50% lower power draw.

¹Affiliated with the Computer Science department at Boston University

²Co-affiliated with the MIT-IBM Watson AI Lab

^{*}Co-first authors

II. BACKGROUND

The firmware and training framework we employ is an evolution of Neuroflight, initially developed by Koch et al. [6], [7]. Neuroflight extends the open-source Betaflight [8] flight-control firmware stack to allow NN models defined in TF1 (v1.13) to be compiled and embedded into the control firmware. This capability enables NN-based flight control. Many problems afflicted the original Neuroflight stack, most prominently, (i) high variance in training and (ii) poor sim-to-real transfer of trained agents. In many cases, trained controllers exhibited worse control and high power consumption than would be expected from their simulated performance. The problem was addressed in follow-up work [9], [10] and attributed to over-engineered rewards and a fundamental lack of smoothness in the trained control policies. By utilizing simplified training rewards and a targeted regularization in policy optimization, CAPS [10] achieved good sim-to-real transfer. Importantly, CAPS enabled significant savings in power consumption, outperforming even fully-tuned PID controllers. However, since CAPS agents are trained in simulation, differences in the dynamics of reality cannot be taken advantage of, thus limiting performance.

Two core limitations of the Neuroflight tool-chain are that (i) it requires NN controllers to be pre-compiled as executable code and statically embedded into the control loop, and (ii) it is keyed to a now obsolete version of the TensorFlow API. The need to pre-compile and embed the controllers into the firmware precludes the ability to modify the controller without compiling and flashing a new firmware. The reliance on obsolete software infrastructure limits the use of newer APIs thus impacting forward compatibility and reproducibility.

III. SWANNFLIGHT SYSTEM FOR LIVE NN CONTROLLER UPDATES

The main goal of this work is to investigate strategies for data-driven live control adaptation. As such, two important sub-goals are formulated as follows. First, we evolve the Neuroflight framework such that modifications to the employed NN controller(s) can be carried out without recompilation. Second, we target live switching capabilities. In other words, updating the NN without interrupting the control loop. In order to achieve the first goal, we re-designed the system to move away from fully frozen NN binaries directly compiled into the firmware. Instead, we add support for *interpretable* NN images via the TensorFlow Lite (TFLite) framework. TFLite provides functions for creating binarized graphs from Keras models, as well as low-level libraries for interpreting and invoking inference over the graphs at runtime. By separating NN controller graphs from the core control loops and making them invocable through the TFLite interpreter, the graphs are no longer an immutable part of the firmware. As such, they can be safely modified at runtime. In particular, it is possible to both (i) update the NN controller weights and (ii) swap-in graphs with different NN architectures. Our updated firmware stack (available online [11]), outlined in Fig. 1, is a fork of Betaflight, and any Betaflight supported

system should be easily transferrable to SwANNFlight, when paired with a compatible transceiver (e.g. an XBee unit).

Given compute and storage limitations of low-power embedded platforms, using TFLite as a NN interpreter is necessary but not sufficient for live data-driven adaptation. While inference can indeed be performed on the onboard flight controller, training onboard is still prohibitively expensive. We mitigate this problem by introducing a point-to-point communication channel with an external ground station. Most importantly, the ground station can be used as a training platform to adapt controllers based on data captured in flight. Our SwANNFlight further integrates with wireless transceiver modules to (i) wirelessly transmit flight data and (ii) accept new NN models to switch to mid-flight.

Wireless communication is handled by a pair of Digi XBee® ZigBee®-PRO radio-frequency modules. The drone communicates observation data to an XBee through a Universal Asynchronous Receiver/Transmitter (UART) port. Similarly, the ground station uses an XBee module to send updated network graphs back to the drone during runtime. The addition of an XBee module connected via the UART port represented the least intrusive set of changes to the existing hardware configuration—and resulting weight and power consumption—of the drone. To ensure the integrity of transmitted data, we implemented a three-phase handshake protocol between the drone and the ground station. The protocol employs cyclic redundancy checks (CRC) to detect errors. Upon graph integrity verification, the drone atomically swaps to invoking the new graph through a buffered copy at the next control cycle. Buffered data is automatically chunked into CRC-validated packets and multiple data transmission rates are supported.

IV. TRAINING FLIGHT CONTROL WITH SWANNFS

Prior work employing the Neuroflight training framework trained RL-based controllers using TF1 [6], [7], [9], [10]. Attempting to deploy these RL-based controllers using our updated stack with TFLite’s interpreter resulted in the control firmware crashing during invocation, due to the operations used by the translated TFv1 NNs. Agents built with TF2, conversely, could be successfully deployed and invoked. This compelled us to update our training stack to TF2.

Transitioning to TF2 introduced a problem for the training pipeline. Prior works [7], [9], [10] train flight-control agents with the OpenAI Baselines [12] implementation of PPO [13]. While reproducible with the software packages and versions reported by the authors, the performance observed with PPO agents in TF1 was not achievable by any of several tested TF2 implementations of PPO, including TF-agents [14], stable-baselines [15] etc., despite using identical network architectures and performing a full hyperparameter search. Algorithms like PPO and TRPO [16] are known to be sensitive to (and even brittle under) implementation specifics [17]–[19], prompting a search for alternatives.

Viable flight-control policies were trainable using a TF2 translation of OpenAI’s Spinning Up [20] PyTorch implementation of DDPG [21]. While vanilla DDPG presented

with similar oscillatory behavior identified in the work on CAPS [10], introducing CAPS regularization to DDPG enabled the training of viable agents in simulation. We found, however, that the performance of DDPG on the control problem at hand exhibited relatively high variance: not all the trained agents were safely flyable. This prompted us to explore alternative formulations which improve upon CAPS defined in the next section.

A. Multiplicative Composition of Optimization Objectives

Prior work has shown that composing multi-objective rewards multiplicatively, instead of linearly, through a geometric mean, where each reward is normalized to the range of $[0, 1]$, can improve training performance and reduce the variance of trained policies [9]. This is analogous to a smooth AND logic operator over different objectives, where the importance of each component signal is preserved. Multiplicative reward composition was shown to help more evenly optimize policies across all objectives. Normalized rewards also offer scale-invariance, preventing individual objectives from overshadowing others. Extending this idea directly to policy optimization, we composed the optimization objectives and regularization terms multiplicatively instead of linearly as in CAPS [10].

For a RL policy $\pi_\theta : S \rightarrow A$, parametrized by θ , that maps states, $s \in S$ to actions $a \in A$ by $a = \pi(s)$, the DDPG policy optimization criteria under the CAPS regularization scheme, $J_{\pi_\theta}^{\text{CAPS}}$ is given as:

$$J_{\pi_\theta}^{\text{CAPS}} = Q_{\pi_\theta}(s, \pi_\theta(s)) - \lambda_T L_T - \lambda_S L_S \quad (1)$$

where $L_T = D(\pi_\theta(s_t), \pi_\theta(s_{t+1}))$

and $L_S = D(\pi_\theta(s_t), \pi_\theta(\bar{s}_t))$ for $\bar{s} \sim N(s, \sigma)$

Under a distance measure D —Euclidean distance in our case— L_T represents a temporal smoothness regularization term that encourages subsequent actions to be similar to each other, and L_S is a spatial smoothness term that encourages similar states to map to similar actions with weights, λ_T and λ_S respectively. A critic, Q_π , estimates the Q-values of state-action pairs for rollouts τ_π under π , i.e.

$$Q_\pi(s, a) = \mathbf{E}_{\tau_\pi} [R(\tau_\pi) | s_0 = s, a_0 = a] \\ = \mathbf{E}_{s'} [r(s, a) + \gamma Q_\pi(s', \pi_\theta(s'))]$$

where s' is the next state reached, $r(s, a)$ defines the per-step reward, and γ is the discount factor.

To compose the policy optimization terms multiplicatively, we first must ensure that they are all within the $[0, 1]$ range. For a reward r in the range $r \in [0, 1]$, scaling the reward by $(1 - \gamma)$ would then result in Q-values being in the range of $[0, 1]$. We also employ temporal and spatial smoothness regularization, normalizing them to the $[0, 1]$ range as well. To mitigate DDPG’s tendency to saturate outputs on either extreme of the output scale, an additional regularization term was added to motivate a reduction in the policy network output prior to the final tanh activation (represented by $\pi^{\cdot-1}$). We shall henceforth refer to the resulting variant of DDPG with multiplicatively composed optimization objectives as

DDPG \times , whose optimization criteria are given by the geometric mean:

$$J_{\pi_\theta} = \sqrt[4]{Q_{\pi_\theta} \left(\frac{w_T}{w_T + L_T} \right) \left(\frac{w_S}{w_S + L_S} \right) \left(\frac{w_A}{w_A + \pi_\theta^{\cdot-1}} \right)} \quad (2)$$

w_T , w_S , and w_A represent values past which to strongly penalize L_T , L_S and $\pi_\theta^{\cdot-1}$ respectively.

To establish a fair comparison with the CAPS approach, we re-implemented CAPS with DDPG as a baseline instead of PPO. Compared to their PPO-TF1 counterparts, trained DDPG policies were more varying in behavior, took longer to train, and have lower performance, resulting in inconsistent behavior when transferred. Adopting the multiplicative composition of the different optimization criteria allowed for much faster training of RL policies, with significantly reduced variance, as demonstrated in Section V-A. DDPG \times introduces key changes in the way regularization is performed to precisely address these issues and consistently trains flight-worthy TF2 agents.

B. Live Adaptation of Flight Controllers with Anchor Critics

Although we were able to train adequately smooth and high-performance agents in simulation, DDPG \times agents’ sensitivity to the reality gap once transferred noticeably impacted control. This offered us an opportunity to utilize the SwaNNFS infrastructure to try and adapt the learned behavior during real-time flight, in order to refine and improve the control response. Note that the possibilities unlocked by the SwaNNFlight firmware go beyond DDPG \times refinement, albeit the combination of DDPG \times and live adaptation is the main focus of our evaluation.

Initial tests showed that naïvely adapting policies learned in simulation to data gathered from live flights could result in swift *catastrophic forgetting*, where policies quickly forgot ‘good’ behavior. This was hypothesized to the biased distribution of experience gained in flight. In simulation, it is possible to constantly train for more aggressive maneuvers without risking physical safety. Conversely, real flight needs to be more conservative. Valid live adaptation must incorporate real flight data while respecting the behavior learned in simulation. We propose adapting agents on two main value criteria: (i) the Q-value on observed experience in flight, just as in DDPG or DDPG \times , and (ii) the Q-value learned on simulation data. The latter is termed as the ‘anchor’ critic and it serves to anchor the policy behavior to the behavior learned in simulation, and the amount of weight and slack offered to it will determine how much policies are allowed to deviate from it in favor of optimizing for data captured during flight.

The anchored policy optimization target, given anchor critic Q-value Q_Ψ , extends Equation 2 as

$$J_{\pi_\theta}^\Psi = \sqrt[5]{Q_{\pi_\theta} Q_\Psi^{w_\Psi} \left(\frac{w_T}{w_T + L_T} \right) \left(\frac{w_S}{w_S + L_S} \right) \left(\frac{w_A}{w_A + \pi_\theta^{\cdot-1}} \right)} \quad (3)$$

with anchor weighting w_Ψ . To ensure that the anchor critic still represents a meaningful Q-value on the policy being

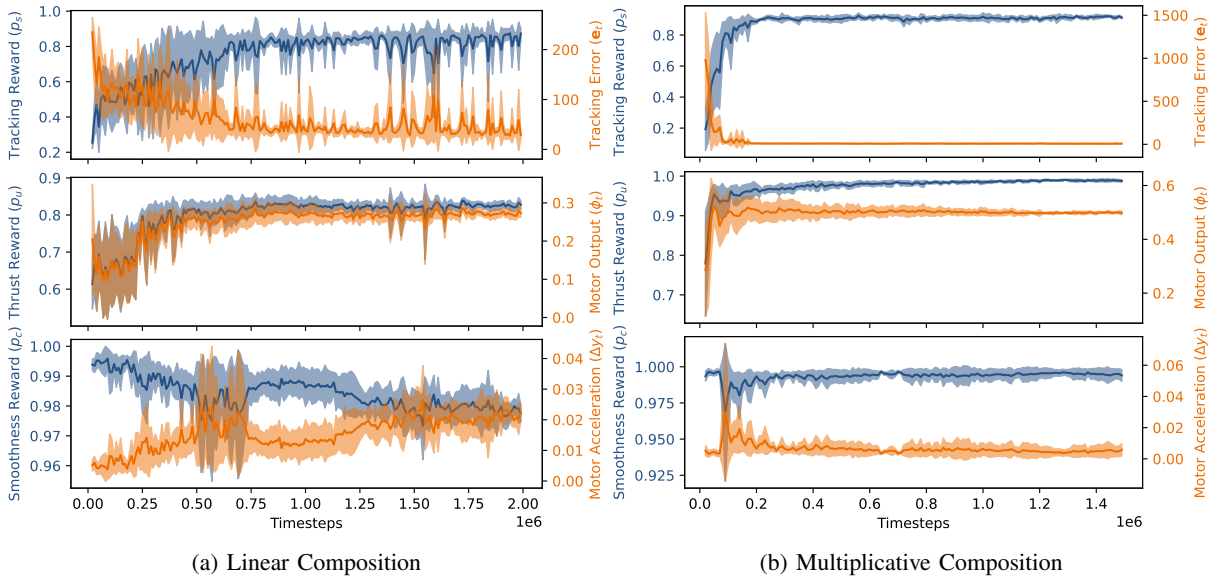


Fig. 2: When comparing multiplicative composition of optimization criteria, as described in Section IV-A, against a CAPS-like [10] linear composition, we observe that the multiplicative composition quickly and significantly reduces learning variance while achieving comparable or better performance metrics where the objectives are to reduce tracking error and motor acceleration, while ensuring that a baseline level of motor actuation is maintained.

optimized, Q_Ψ continues to be updated during training, following the typical DDPG critic update, using the current adapted policy but only on data from the replay buffer generated during simulated training. The live-flight Q-value Q_π is conversely trained only on live flight data.

V. EVALUATION AND DISCUSSION

The novel infrastructure offered by the SwaNNFS enabled us to develop and test practical ways to adapt agents while a quadrotor is in flight. The obstacles presented in achieving consistent and safe live-adaptation lead to our proposed methods. We therefore support our choices by (1) establishing the improvements of multiplicative composition over CAPS implemented in DDPG, via an ablation study in Section V-A; (2) showing the effectiveness and general applicability of anchor critics via exploration on a toy problem in Section V-B; (3) evaluating how live adapting with and without anchors affects safety, smoothness, and performance on the real drone system in Sections V-C and V-D; and (4) offering theoretical arguments motivating our method in Section V-E. Finally, we discuss known limitations with respect to drone control and the general cost of using anchors in Section V-F.

Two key performance metrics are used in policy evaluation. (1) Tracking accuracy is measured using the Mean Absolute Error (MAE). (2) Smoothness is computed by taking the Fast Fourier Transform (FFT) of the actuation commands, and then computing Sm as defined by Equation 4 in [10]. The smoothness measure is small for a smooth controller and large for a noisy and jerky controller. Appendix B in the supplementary material [11] provides details on hyperparameters used, along with code for SwaNNflight and DDPG \times RL training.

A. Multiplicative Composition of Optimization Criteria

We trained controllers in simulation using CAPS-like [10] linear loss composition against multiplicative loss composition, shown in Equation 2, in order to demonstrate the improvements offered by DDPG \times . In an effort to reproduce the same level of performance achieved with the TF1 OpenAI baselines implementation of PPO, as documented in the CAPS work [10], with our TF2 implementation of DDPG, we conducted extensive tests with different weighting parameters, both for the CAPS regularization terms as well as the training rewards. Even with our best set of hyperparameters, however, variance in trained performance remained high and performance did not match the quality previously achievable on the TF1 framework (see Appendix B on our website [11] for details). We were not able to achieve comparable performance with any of the popular contemporary Q-learning based algorithms – DDPG, SAC, or TD3. We mainly focused on DDPG (motivated by our hyperparameter search) as a starting point to explore techniques to further improve and stabilize its performance. By adopting the multiplicative composition of terms described in Section IV-A, we were able to achieve higher performance with less tuning and significantly reduced variance, as shown in Fig. 2. The results presented in the figure compare 6 independently trained agents for both linear and multiplicative composition. Weights shown in Equation 2 are chosen individually so that undesirable performance on any criterion would evaluate to values near 0.

B. Testing Anchors on Inverted Pendulum

In this and the following sections, we evaluate the behavior of agents refined using anchor critics when fine-tuning controllers to establish the effectiveness of the approach in terms of (i) impact on policy stability, (ii) forgetfulness,

and (iii) ability to preserve tracking performance while better regularizing policies for smoother, less power-hungry behavior.

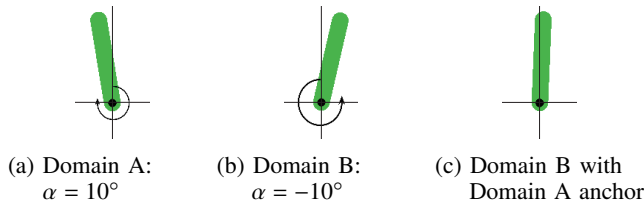


Fig. 3: Policies in (a) and (b) are initially trained to lean an inverted pendulum at their respective angle α . While in (c) the anchor-critic from the Domain A causes the resultant fine-tuned policy to hold the pendulum straight-up with no significant lean. Fig.4 demonstrates an example of how the pendulum states evolve with time before and after adaptation.

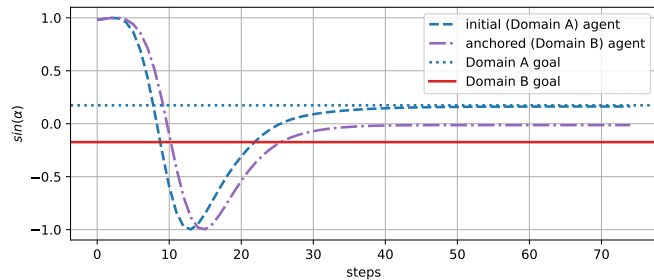


Fig. 4: The \sin of the inverted pendulum’s angle α over time starting from $\alpha = 90^\circ$ for a DDPG agent trained initially on Domain A as per Fig. 3a, and then adapted to Domain B with Domain A anchors as per Fig. 3c. Note that initial training allows the agent to stably balance the pendulum to approximately 10° while adaptation results in the agents driving the pendulum to approximately 0° .

To test the general viability of anchor critics, we implemented them in three popular contemporary RL algorithms: DDPG [21], SAC [22], and TD3 [23] and tested them on a modified inverted pendulum problem. The typical goal of the task is to stabilize a torque-controlled pendulum vertically upright, but we instead target holding the pendulum at a specified angle. Agents were instead trained to lean an inverted pendulum to the left while upright (Fig. 3a). Those agents were then retrained to lean right, but this time by using anchors from Domain A, agents were also incentivized to lean left. The resulting policies were observed to learn to balance the pendulum straight-up with no lean since the new rewards condition the ‘live’ critic to motivate the policy to lean right, while the anchor critic simultaneously preserves leaning left (Fig. 3c). An overview of this problem is provided in Fig. 3. Fig. 4 demonstrates an example of this behavior for a DDPG agent. Additional data for more agents and for agents trained with different algorithms are available on our website [11] and are also discussed in the companion video for this paper.

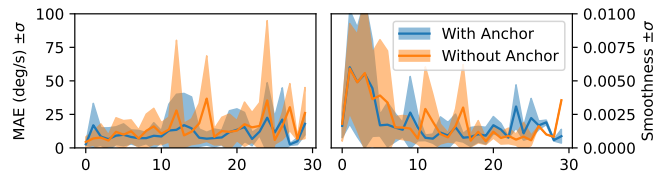


Fig. 5: Shown here is how MAEs and smoothness evolve with adaptation steps, with and without anchors. In both cases smoothness improves, however, without anchors, tracking errors often diverge wildly as catastrophic forgetting occurs and the quadrotor fails to follow larger control inputs. With anchors, error is bounded and remains in controllable range.

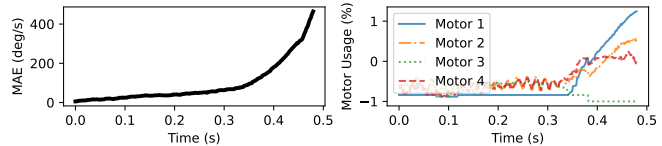


Fig. 6: A snapshot of instability of the drone during an adaptation run without anchors when facing large deltas in control input. Observe how error increases exponentially as the drone controller enters an unrecoverable state (and eventually hitting the safety net in our tests – as shown in this paper’s companion video).

C. Catastrophic Forgetting and Safety Concerns in Adaptation without Anchors

Before testing adaptation in live, unconstrained flight, we first conducted a series of tests in a controlled lab environment where the drone was attached to a light tether to restrain it in the event of a catastrophic loss of control, without being a hindrance to flight. These tests consisted of fine-tuning a well-trained controller from simulation on the real platform while giving it typically small control targets (< 50 deg/s) and occasionally requesting control in excess of that (> 100 deg/s). Without anchors preserving agents’ performance on larger control inputs—like those experienced during the simulated training—the live agents were observed to forget how to maintain tracking when receiving large inputs, though sometimes regaining control, and often losing it again, as seen in Fig. 5. This also results in a sudden loss of control where errors would quickly snowball and motor actuation rises sharply, risking damage to the drone. Fig. 6 demonstrates how, when commanding attitudes not seen for a while during live-flight adaptation, agents could very quickly lose control (observed from MAEs increasing quickly and exponentially) – which we attributed to overfitting over the relative homogeneity of the live-flight training data. Anchors help avoid this problem.

D. Live Adaptation During Unconstrained Flight

As a final test, we test our anchored live adaptation method in unconstrained flight outdoors (with adequate safety precautions). Shown in Fig. 7 is a comparison of control signals before and after 15 adaptation steps. Motor usage is reduced significantly, resulting in improved control smoothness and almost a 50% reduction in power consumption, with comparable MAEs to agents trained in simulation. This is

further demonstrated in Table I, which examines how MAE, smoothness, and current draw change through adaptation.

TABLE I: Errors and power consumption in flight before and after 15 steps of live adaptation

	Before Adaptation	After Adaptation
Amperage ↓	13.7 ± 8.47	7.24 ± 3.97
Mean Average Error ↓	12.55 ± 12.22	14.13 ± 5.21
Smoothness $\times 10^4$ ↓	12.6 ± 0.98	5.85 ± 0.96

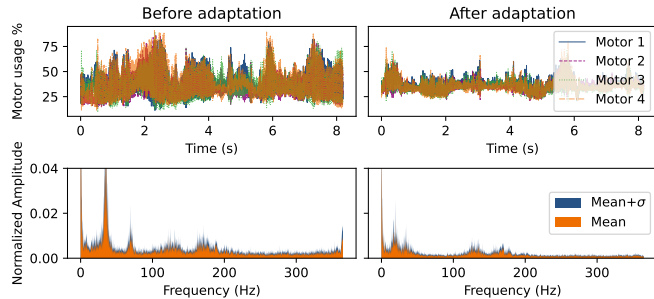


Fig. 7: Comparisons of motor usage during flight and corresponding FFTs demonstrate the improvement in smoothness after adaptation, as noted from the reduction in high-frequency components on the FFT amplitude plot. While the motor usage plot samples a single trajectory for clarity, the FFTs are averaged over multiple adaptations to demonstrate repeatability.

E. A Case Against Mixing Replay Buffers During Adaptation

It may seem reasonable, as a first-pass solution, to fine-tune agents for real flight by mixing simulated and real data during fine-tuning. However, theoretically, training a single critic with a mixture of data from two separate environments would violate the RL algorithms’ Markovian assumption. The different environments have different dynamics so their implicit transition functions would depend on a now hidden state not represented in our state space, namely which environment it comes from. One could possibly include this, however this would necessitate a change in the agents’ input structure and corresponding controller NN model architecture. We therefore instead opted to maintain two separate Q-value functions and replay buffers. Separating the Q-value functions also enables weighing how much actors ‘care’ about optimizing one value function over the other, allowing us to tune how much we trade off stability over adaptability and vice versa.

F. Known Limitations

Both SwaNNFS and the anchored learning techniques discussed in this work demonstrate a clear utility in sim-to-real control transfer and live adaptation of learned controllers on a compute-constrained platform. However, even with the improvements we demonstrate, we are not yet able to surpass the performance of the PPO algorithm on TF1 with any of the algorithms tested so far on TF2. Furthermore, while anchors clearly help improve control smoothness without resulting in catastrophic forgetting, the adapted agents were not observed to improve their tracking performance, even though this remained the key learning objective of the policy

optimization. It is as yet unclear as to whether this is simply a limitation of the DDPG algorithm (or our specific implementation), or a matter of how the regularization was tuned. Finally, even though we demonstrate that anchors can be helpful in preserving behaviors from one environment when fine-tuning an agent on another, the optimization structure forces a performance compromise. While this helps prevent forgetting, it also prevents policies from adopting substantially new and potentially more effective behaviors. This is by design, of course, but in cases where domain gaps are large, the very stability offered by the anchor critics may significantly compromise fine-tuning of behavior and could result in policies that are ill-suited for both the initial and transferred domain. Another limitation is our use of a saved replay buffer from simulation to evaluate anchor critics. While this worked in our experiments, we suspect that keeping the simulation in the loop might allow for anchors to better represent simulation performance.

VI. RELATED WORK

Work exploring controller-based live-adaptivity can be divided into either model-based or model-free approaches. In classical control theory [24], given a family of models, adaptation is defined as being synonymous with identifying the parameters for the optimal model from observations. Techniques based on this theory have been used for quadrotor control as well [25]. More recent advances have sought to tackle adaptation in more challenging control problems by employing model-based reinforcement learning [26]. Model-based RL techniques are, however, constrained by difficulties in accurately modeling the dynamics of real systems. Meta RL has also been proposed as a model-free solution for adaptivity, where policies are trained to adapt to different environments [27]–[29]. However, these techniques rely on being able to identify and vary simulator parameters to maximally cover a wide array of possible distributional shifts in order to enable policies to adapt to real-life scenarios. They are therefore limited by how much simulated environments can represent unexpected shifts in the dynamics of reality. Other methods directly employ RL, either via on-board compute, or via immediate communication, however, safety is often a concern under arbitrary policies. Cheng et al. [30] attempt to address this by allowing only safe exploration, but again rely on being able to model safety criteria. There are, of course, more direct optimization tricks too, such as the idea of keeping policies within a ‘trust region’ during optimization, to improve stability and prevent large changes in behavior [13], [16]. While this constraint can be tuned to adapt policies only within a trust region, progressive optimization could still result in significant deviation.

VII. CONCLUSION

Our work introduced the Swappable Neural Network Flight control System (SwaNNFS), a framework for enabling live adaptation of neural network based flight control for drones, or indeed any other Betaflight compatible platform. Our full-stack software enables ground-to-drone

communication so that agents' observations during flight can be transmitted back to a ground-station for controller adaptation, with the adapted controllers being transferred back to the drone, which the drone can seamlessly swap to without compromising the control loop. We also introduce a novel framing of the RL optimization criteria, and introduce anchor critics as a tool to stabilize sim-to-real adaptation. As we demonstrate, the introduction of anchor critics can significantly improve behavior retention while still giving policies enough slack to adapt themselves to new data. This was shown to substantially improve control smoothness and reduce power consumption without degradation in control input tracking performance.

REFERENCES

- [1] A. R. Mahmood, D. Korenkevych, G. Vasan, W. Ma, and J. Bergstra, "Benchmarking reinforcement learning algorithms on real-world robots," *Conference on Robot Learning*, 2018. [Online]. Available: <http://arxiv.org/abs/1809.07731>
- [2] F. Sadeghi, A. Toshev, E. Jang, and S. Levine, "Sim2Real view invariant visual servoing by recurrent control," *CoRR*, vol. abs/1712.07642, 2017.
- [3] A. Molchanov, T. Chen, W. Hönig, J. A. Preiss, N. Ayanian, and G. S. Sukhatme, "Sim-to-(multi)-real: Transfer of low-level robust control policies to multiple quadrotors," *International Conference on Intelligent Robots and Systems*, 2019. [Online]. Available: <http://arxiv.org/abs/1903.04628>
- [4] Y. Duan, X. Chen, R. Houthoofd, J. Schulman, and P. Abbeel, "Benchmarking deep reinforcement learning for continuous control," in *Proceedings of the 33rd International Conference on International Conference on Machine Learning - Volume 48*, ser. ICML'16. JMLR.org, 2016, pp. 1329–1338.
- [5] W. Koch, "Flight controller synthesis via deep reinforcement learning," 2019.
- [6] W. Koch, R. Mancuso, R. West, and A. Bestavros, "Reinforcement learning for UAV attitude control," *ACM Transactions on Cyber-Physical Systems*, 2018.
- [7] W. Koch, R. Mancuso, and A. Bestavros, "Neuroflight: Next generation flight control firmware," *CoRR*, vol. abs/1901.06553, 2019. [Online]. Available: <http://arxiv.org/abs/1901.06553>
- [8] "Betaflight." [Online]. Available: <https://betaflight.com/>
- [9] S. Mysore, B. Mabsout, K. Saenko, and R. Mancuso, "How to train your quadrotor: A framework for consistently smooth and responsive flight control via reinforcement learning," *ACM Transactions on Cyber-Physical Systems (TCPS)*, vol. 5, no. 4, pp. 1–24, 2021.
- [10] S. Mysore, B. Mabsout, R. Mancuso, and K. Saenko, "Regularizing action policies for smooth control with reinforcement learning," in *2021 IEEE International Conference on Robotics and Automation (ICRA)*, 2021, pp. 1810–1816.
- [11] "Swappable neural network flight control system homepage." [Online]. Available: <https://github.com/BU-Cyber-Physical-Systems-Lab/SwaNNFS>
- [12] P. Dhariwal, C. Hesse, O. Klimov, A. Nichol, M. Plappert, A. Radford, J. Schulman, S. Sidor, Y. Wu, and P. Zhokhov, "Openai baselines," <https://github.com/openai/baselines>, 2017.
- [13] J. Schulman, F. Wolski, P. Dhariwal, A. Radford, and O. Klimov, "Proximal policy optimization algorithms," *arXiv:1707.06347*, 2017.
- [14] S. Guadarrama, A. Korattikara, O. Ramirez, P. Castro, E. Holly, S. Fishman, K. Wang, E. Gonina, N. Wu, E. Kokioyopoulou, L. Sbaiz, J. Smith, G. Bartók, J. Berent, C. Harris, V. Vanhoucke, and E. Brevdo, "TF-Agents: A library for reinforcement learning in tensorflow," 2. [Online]. Available: <https://github.com/tensorflow/agents>
- [15] A. Hill, A. Raffin, M. Ernestus, A. Gleave, A. Kanervisto, R. Traore, P. Dhariwal, C. Hesse, O. Klimov, A. Nichol, M. Plappert, A. Radford, J. Schulman, S. Sidor, and Y. Wu, "Stable baselines," 2018.
- [16] J. Schulman, S. Levine, P. Abbeel, M. Jordan, and P. Moritz, "Trust region policy optimization," in *Proceedings of the 32nd International Conference on Machine Learning*, Lille, France, 07–09 Jul 2015.
- [17] P. Henderson, R. Islam, P. Bachman, J. Pineau, D. Precup, and D. Meger, "Deep reinforcement learning that matters," in *Proceedings of the AAAI Conference on Artificial Intelligence*, vol. 32, no. 1, 2018.
- [18] R. Islam, P. Henderson, M. Gomrokchi, and D. Precup, "Reproducibility of benchmarked deep reinforcement learning tasks for continuous control," *arXiv preprint arXiv:1708.04133*, 2017.
- [19] L. Engstrom, A. Ilyas, S. Santurkar, D. Tsipras, F. Janoos, L. Rudolph, and A. Madry, "Implementation matters in deep rl: A case study on ppo and trpo," in *International Conference on Learning Representations*, 2020.
- [20] J. Achiam, "Spinning Up in Deep Reinforcement Learning," 2018.
- [21] T. P. Lillicrap, J. J. Hunt, A. Pritzel, N. Heess, T. Erez, Y. Tassa, D. Silver, and D. Wierstra, "Continuous control with deep reinforcement learning," *International Conference on Learning Representations*, 2016.
- [22] T. Haarnoja, A. Zhou, P. Abbeel, and S. Levine, "Soft actor-critic: Off-policy maximum entropy deep reinforcement learning with a stochastic actor," *International Conference on Machine Learning (ICML)*, 2018.
- [23] S. Fujimoto, H. Hoof, and D. Meger, "Addressing function approximation error in actor-critic methods," in *International Conference on Machine Learning*, 2018, pp. 1587–1596.
- [24] B. Pasik-Duncan, "Adaptive control," *IEEE Control Systems*, vol. 16, pp. 87–, 1996.
- [25] M. Schreier, "Modeling and adaptive control of a quadrotor," 08 2012.
- [26] Y. Song, A. Mavalankar, W. Sun, and S. Gao, "Provably efficient model-based policy adaptation," in *ICML*, 2020.
- [27] K. Arndt, M. Hazara, A. Ghadirzadeh, and V. Kyrki, "Meta reinforcement learning for sim-to-real domain adaptation," in *2020 IEEE International Conference on Robotics and Automation (ICRA)*, 2020, pp. 2725–2731.
- [28] A. Nagabandi, I. Clavera, S. Liu, R. S. Fearing, P. Abbeel, S. Levine, and C. Finn, "Learning to adapt in dynamic, real-world environments through meta-reinforcement learning," *arXiv: Learning*, 2019.
- [29] O. M. Andrychowicz, B. Baker, M. Chociej, R. Józefowicz, B. McGrew, J. Pachocki, A. Petron, M. Plappert, G. Powell, A. Ray, J. Schneider, S. Sidor, J. Tobin, P. Welinder, L. Weng, and W. Zaremba, "Learning dexterous in-hand manipulation," *The International Journal of Robotics Research*, vol. 39, no. 1, pp. 3–20, 2020. [Online]. Available: <https://doi.org/10.1177/0278364919887447>
- [30] R. Cheng, G. Orosz, R. M. Murray, and J. W. Burdick, "End-to-end safe reinforcement learning through barrier functions for safety-critical continuous control tasks," *Proceedings of the AAAI Conference on Artificial Intelligence*, vol. 33, no. 01, pp. 3387–3395, Jul. 2019. [Online]. Available: <https://ojs.aaai.org/index.php/AAAI/article/view/4213>
- [31] "Rl hyperparameter zoo," <https://github.com/araffin/rl-baselines-zoo/tree/master/hyperparams>, 2018.

A. *SwaNNFlight System Transceiving Metrics*

Using the Transceiving framework and hardware described in Section III, i.e MATEK-F722 controller equipped with ZigBee®-PRO radio-frequency modules, transmission and switching time for NNs were measured. The control networks used in this work use two hidden layers with 32 neurons each. We employ a transmission baudrate of 115200 to send NNs of 8mb, which takes 11 s to transfer between the ground station and the drone – receiving is handled in parallel to the flight control, so the drone is able to remain fully operational while waiting for a new network. When a network is received, switching to the new NN controller takes 134 ms. During flight, the drone also transmits state observations of 59 bytes back to the ground station, transmitting 244 observations per second.

B. *Hyper-parameter search*

We conducted a hyper-parameter search and a correlation factor analysis using 4 different prominent RL algorithms – PPO, DDPG, SAC and TD3 – for the quadrotor attitude control problem mainly considered in this paper. The list of tested hyper-parameters and their corresponding correlations to the training reward are presented in Tables III, IV, V and VI respectively. Our hyper-parameter choices were informed by common values used to achieve the best performance across various benchmark Gym environments [31].

Table II meanwhile compares the training performances of each of the algorithms, as well as DDPG \times which we introduce in this work, after 300000 training steps (corresponding to a quarter of our typical training time and the time by which DDPG \times typically starts to plateau), but on a slightly modified version of the problem – where agents are only required to minimize tracking error, without worrying about other characteristics such as control smoothness. This, we found, was typically a good starting point for tuning algorithms’ hyper-parameters and to determine if they are capable of addressing the underlying control problem. As the data demonstrates, all the tested algorithms perform significantly worse than DDPG \times .

While the relative performance metrics appear similar across DDPG, PPO, SAC and TD3, there are critical differences in the quality of the behaviors being learned, which in turn impacts the ability of the algorithms to further improve agents’ performances. As shown in Fig. 9, the tested TF2 implementation of PPO does not behave similarly to the modified OpenAI Baselines [12] TF1 version used in previous work. [7], [9], [10]. Where the PPO based on Baselines learns to track the control signals well, albeit with high variance in the motor actuation (since smoothness is not being trained for), the TF2 implementation saturates the motor commands at the maximum, thus effectively doing nothing to control the drone’s attitude. This still generates some reward, since the training environment predominantly consists of smaller (but more frequently varying) control angular velocities. The

problem with this, however, is that this behavior seems to be a local optima that is difficult for the algorithms to recover from to further improve performance.

When considering alternatives to PPO, we experimented with Q-learning-based DDPG, SAC and TD3. As shown in Fig. 10, we observed that TD3 would often fall into similar trappings as PPO, with the motor outputs becoming saturated at maximum actuation. While DDPG was slower to learn (often performing worse than SAC), crucially, it did not saturate and would in fact consistently try to maintain control through more nuanced use of the motors – an extreme but illustrative case is shown in Fig. 10. Given our results, while SAC would have been preferable as a starting point based on the typical rewards achieved, the fact remained that training SAC was approximately 1.5 times slower than DDPG for relatively marginal gains, making it a less attractive option for iterating. DDPG was therefore deemed the best contender with which to experiment on our proposed multiplicative policy optimization. In our tests, agents which achieve an average reward of more 0.8 were typically responsive enough to control in real flight.

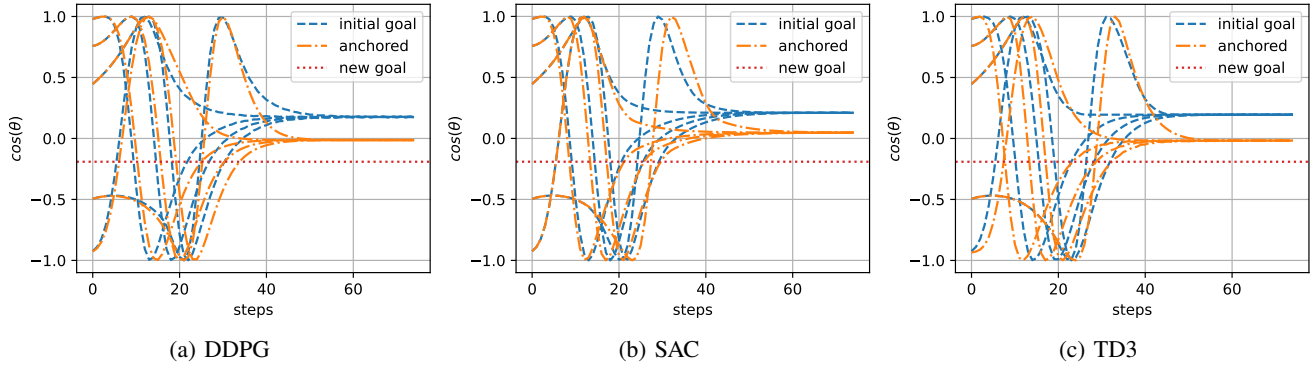


Fig. 8: Evolution of the angle ($\sin(\theta)$) of an inverted pendulum over time for policies trained with anchor-critics tested on DDPG, SAC and TD3. There are 5 different test runs per goal, and the angle of the pendulum is initialized at random. All 3 anchored algorithms consistently learn to point to 0 rad, thus maintaining a good compromise between our initial goal and our new goal.

TABLE II: This table shows the performance of the different RL algorithms over the aforementioned environment. Training ends after invoking the environment 300,000 times and is tested 5 times for every hyperparameter sample. The reward value is then computed for every sample of hyperparameters of which there are at least 10 samples per algorithm. Step times are reported for a desktop running Ubuntu v 18.04 with an Intel Core i7-7700 CPU (no GPU optimization is used since training is primarily CPU limited).

Algorithm	DDPG \times	DDPG	PPO (TF2)	SAC	TD3
Reward	0.89 ± 0.033	0.38 ± 0.13	0.36 ± 0.11	0.40 ± 0.12	0.37 ± 0.11
Max Reward	0.93	0.59	0.61	0.63	0.57
Step time (s)	9.6×10^{-3}	9.6×10^{-3}	3.6×10^{-3}	1.44×10^{-2}	1.2×10^{-2}

TABLE III: TF2 PPO paramater/reward correlations

Parameter	Correlation	Tested Values
Clip ratio	0.098	[0.0, 0.05, 0.1, 0.2]
γ	-0.100	[0.8, 0.9, 0.95, 0.99]
Policy learning rate	0.679	[1e-4, 5e-4, 1e-3, 3e-3, 5e-3]
Value learning rate	0.255	[1e-4, 5e-4, 1e-3, 3e-3, 5e-3]
lam	0.056	[0.9, 0.97, 0.99, 0.995]

TABLE IV: DDPG paramater/reward correlations

Parameter	Correlation	Tested Values
Replay buffer size	-0.156	[100 000, 500 000, 1000 000, 5000 000]
γ	-0.161	[0.8, 0.9, 0.95, 0.99]
Polyak	0.203	[0.5, 0.9, 0.95, 0.99, 0.995]
Policy learning rate	-0.211	[1e-4, 5e-4, 1e-3, 3e-3, 5e-3]
Critic learning rate	-0.676	[1e-4, 5e-4, 1e-3, 3e-3, 5e-3]
Batch size	-0.142	[50, 100, 200, 400]
Action noise	-0.691	[0.01, 0.05, 0.1, 0.2]

TABLE V: SAC paramater/reward correlations

Parameter	Correlation	Tested Values
Replay buffer size	-0.088	[100 000, 500 000, 1000 000, 5000 000]
γ	0.272	[0.8, 0.9, 0.95, 0.99]
Polyak	0.102	[0.5, 0.9, 0.95, 0.99, 0.995]
Learning Rate	-0.256	[1e-4, 5e-4, 1e-3, 3e-3, 5e-3]
α	0.356	[0.01, 0.05, 0.1, 0.2]
Batch size	0.866	[50, 100, 200, 400]

TABLE VI: TD3 paramater/reward correlations

Parameter	Correlation	Tested Values
Replay buffer size	0.516	[100 000, 500 000, 1000 000, 5000 000]
γ	0.479	[0.8, 0.9, 0.95, 0.99]
Polyak	0.007	[0.5, 0.9, 0.95, 0.99, 0.995]
Policy learning rate	-0.430	[1e-4, 5e-4, 1e-3, 3e-3, 5e-3]
Critic learning rate	0.023	[1e-4, 5e-4, 1e-3, 3e-3, 5e-3]
Batch size	0.118	[50, 100, 200, 400]
Act noise	0.313	[0.01, 0.05, 0.1, 0.2]

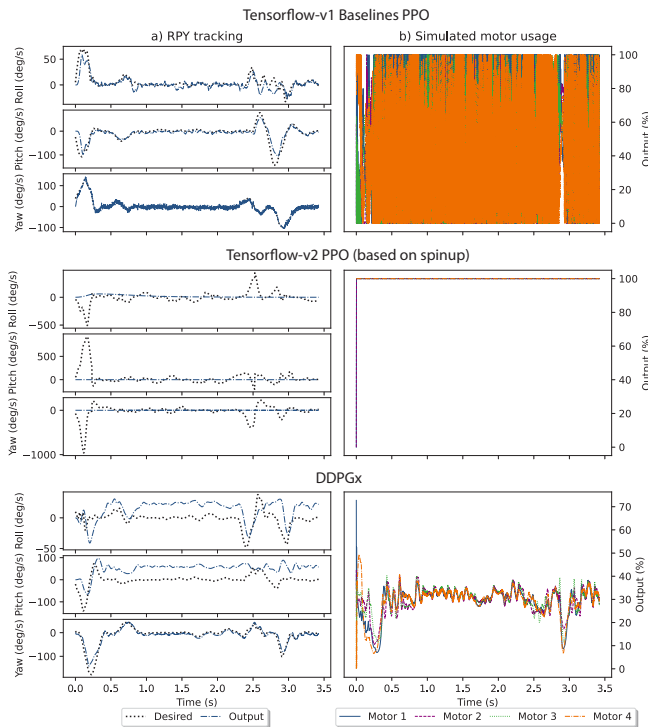


Fig. 9: A snapshot of PPO and DDPG \times agents after 300,000 training steps acting in their training environment. Attitude control elements are split into Yaw, Pitch, and Roll in the left column. On the right are the outputs generated by the agents while attempting to follow the control inputs. Without smoothness considerations, within 300,000 steps, Baselines PPO performs very well on tracking while outputting actions with high variability (as is shown in previous works [10], [9]). Conversely, the TF2 implementation of PPO fails to learn useful behavior across hyper-parameters. DDPG \times , which we introduced in this work, is able to reasonably follow the target while maintaining smooth outputs and continues to improve as training progresses.

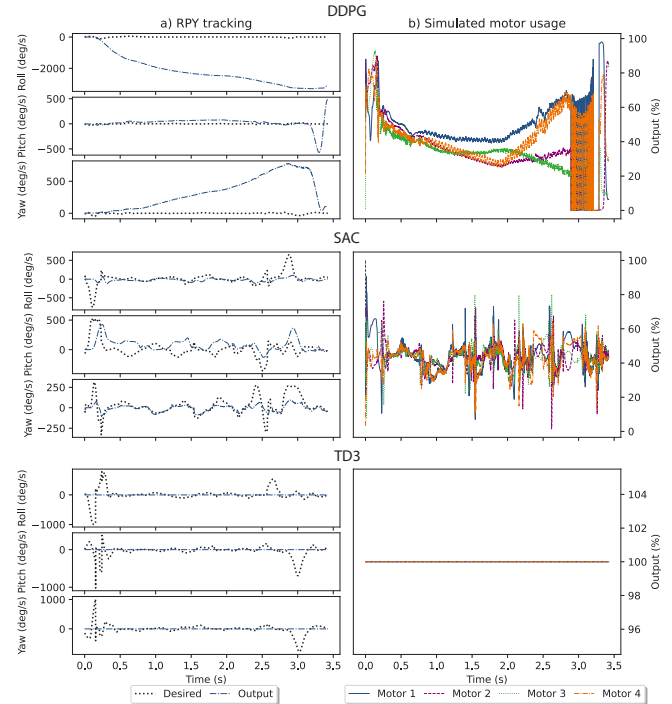


Fig. 10: For the three DDPG-based algorithms, we observe clear dissimilarities in the quality of the policies learned, based on input tracking and motor usage. Entropy regularization employed in SAC allows trained agents to achieve relatively reasonable performance on both tracking and motor usage, but the algorithm was noted to not improve further with more training, likely due to the same regularization that initially helps preventing large responses, thus preventing the algorithm from learning to track more aggressive maneuvers. TD3 behaves similarly to the TF2 PPO, in that it tends to saturate at various local optima, outputting extreme values. DDPG, on the other hand, demonstrates some tracking capabilities can varies its control output drastically when close to the setpoint, similar in behavior to Baselines PPO. Given these three candidate algorithms and their relative benefits and drawbacks, we chose to modify DDPG as it runs faster than SAC and was capable of achieving good tracking performance. While DDPG itself was not consistently reliable, DDPG \times , with our proposed improvements, was repeatable and controllable.